



## Admittance Modeling of the Power System with DFIG based WECS for IGE Analysis

Srikanth Velpula<sup>1</sup> and R. Thirumalaivasan<sup>2</sup>

<sup>1</sup>Research Scholar, School of Electrical Engineering, Vellore Institute of Technology Vellore (Tamilnadu), India.

<sup>2</sup>Associate Professor, School of Electrical Engineering, Vellore Institute of Technology Vellore (Tamilnadu), India.

(Corresponding author: R. Thirumalaivasan)

(Received 15 May 2020, Revised 25 June 2020, Accepted 05 July 2020)

(Published by Research Trend, Website: [www.researchtrend.net](http://www.researchtrend.net))

**ABSTRACT:** The use of admittance/impedance model based method is attracting researchers for Subsynchronous Resonance (SSR) screening studies. The incorporation of converter based systems in to the grid can change the overall admittance/impedance of the system, which may cause reduction in the damping at SSR frequency. In this paper, we present a simple and attractive procedure for obtaining the admittance model of a system. Further, the admittance model of modified IEEE First Bench Mark (FBM) model with the inclusion of Doubly-Fed Induction Generator based Wind Energy Conversion System (DFIG based WECS) is developed. With the admittance model, the analysis on Induction Generator Effect (IGE) of DFIG based WECS is carried out for different wind speeds and compensation levels. The admittance analysis results indicate, the conductance offered by the network to the SSR frequency components is large at high wind speed and high compensation levels. In IGE analysis, the SSR frequency and conductance offered by the network to the SSR frequency components are estimated. To show the effectiveness and significance of the admittance model based analysis on IGE, the results are correlated with the eigenvalue analysis. The analyses show that, the variation in network conductance of admittance analysis indicates variation in the real part of eigenvalues and the variation in SSR frequency of admittance analysis indicates variation in the imaginary part of eigenvalues. The results demonstrate that, the high conductance offered by the network to SSR frequency components indicate the severity of IGE.

**Keywords:** Admittance model based analysis, Doubly-Fed Induction Generator (DFIG), Eigenvalue analysis, Induction Generator Effect (IGE), Subsynchronous Resonance (SSR), and Wind Energy Conversion System (WECS).

### I. INTRODUCTION

The incorporation of power electronic based systems into the power system raises the complexity in estimation of the system stability [1-10]. The impedance and admittance models of the grid and Voltage Source Converter (VSC) are useful for the assessment of stability on converter-grid interactions [1, 2]. In addition, the stability of the system may ensure with the modifications in input admittance through VSC control parameters [1]. The impedance models of VSC and grid are modeled as Norton and Thevenin equivalent impedances to assess the stability and resonance conditions of the system. The impedance/admittance model based stability analysis is proposed by obtaining the ratio of source to load based on Nyquist criterion [2]. The positive and negative sequence impedance models of grid connected VSC are proposed to assess the stability of balanced three-phase converter based systems [3].

Fan and Miao [4] demonstrate the application of impedance-based Nyquist stability for Subsynchronous Resonance (SSR) analysis in Doubly-Fed Induction Generator based Wind Energy Conversion System (DFIG based WECS). The impedance model of a DFIG based WECS is developed analytically for the SSR analysis [5]. A comparative study between impedance based analysis and eigenvalue analysis is elaborated in [6]. Results indicate the effectiveness of each method in

estimating the system stability; however, the lack of observability on certain states needs further investigation of impedance based analysis at different subsystems. Recently, the impedance model based frequency scanning techniques are used to study the stability of Subsynchronous Oscillations/Subsynchronous Interactions (SSO/SSI) [7-10]. The SSR stability criterion based on an aggregated RLC circuit model is developed from the impedance models [7]. From the RLC circuit parameters the SSR characteristics are presented quantitatively. The SSO characteristics in a multiple DFIGs connected with VSC-HVDC system are explained with impedance models and realized by RLC resonance circuit [8]. The risk of SSR is assessed through the development of impedance models consisting multiple VSC based systems in a cluster [9].

For the large network consisting number of generation units and transmission lines, the individual impedance models are developed and integrated appropriately [7, 10]. Based on the stability criterion used the impedance models are represented as a lumped impedance viewing from the driving point [10] or split into two impedance models acting as a load and a source [2]. The impedance model based Nyquist-criterion approach is cumbersome to apply to a meshed power network which has many wind farms. Also, the method based on the Nyquist criterion is a qualitative method and may not provide accurate findings on SSR damping and

frequency [2, 4, 7, 10]. The calculation of eigenvalues requires the detailed state space representation of the whole system including electrical and mechanical subsystems [6, 11]. In literature, the complex torque/damping torque based frequency scanning methods utilize the system admittance functions for SSR analysis [11-16].

Recently, the use of admittance models is increasing to predict the stability of converter based systems connected to the grid [17-18]. Subsequently, the admittance model results validate through time domain simulations [17] and frequency scan methods [18]. Investigation shows that, the stability of the system is accurately estimated using eigenvalues computed from the system admittance function compared to Nyquist and Bode plots. In this context, we present a methodology to develop the admittance model of a system and using the admittance model based methods for SSR analysis requires the validation through existing conventional methods like eigenvalue analysis. Subsequently, the correlation with eigenvalue analysis indicates the usefulness of admittance models in estimating the SSR characteristics.

In this paper, we introduce a simple and attractive procedure for obtaining admittance model of the power system. The procedure is applied to develop the admittance model of the power system consisting DFIG based WECS connected to infinite bus through series compensated transmission line. Further, the admittance model based approach is used for the analysis of Induction Generator Effect (IGE) and correlated with the eigenvalue analysis. The overall admittance model of the system is developed viewing from the infinite bus. The contributions and features of the paper include:

- A Step-by-step procedure to develop the admittance model of the power system.
  - Estimation of SSR frequency and conductance offered by the network to SSR frequency components using admittance model.
  - Admittance model based analysis on IGE at different wind speeds and compensation levels.
  - Correlating the admittance analysis with the eigenvalue analysis.
  - The admittance modeling procedure is useful to obtain the admittance models of large power system consisting number of generating systems and transmission lines.
- The structure of the paper is as follows: the modeling details of the test system are described in Section II. The admittance modeling procedure and test system admittance model is presented in Section III. Section IV presents the IGE analysis through admittance model and the correlation with the eigenvalue analysis. The conclusions are outlined in Section V.

## II. TEST SYSTEM DESCRIPTION AND MODELING

The single line diagram of the test system adopted to analyze the IGE is shown in Fig. 1 (modified IEEE First Bench Mark (FBM) model [19]). The test system consists of DFIG based WECS and synchronous generator, which are connected through short lines at point of common coupling (PCC) as shown in Fig. 1. The series compensated long transmission line is connected from PCC to infinite bus. To analyze the IGE effect of DFIG based WECS, the synchronous generator is modeled as a voltage source behind the reactance

[11]. The DFIG is modeled in  $dq$ -frame using generator convention, in which q-axis leads the d-axis [11].

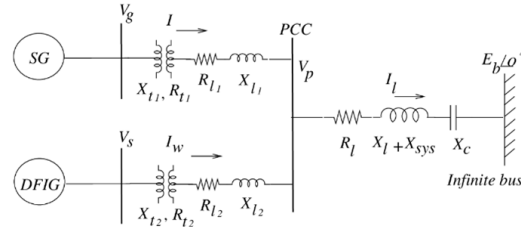


Fig. 1. Single line diagram of the test system.

The DFIG based WECS comprises wind turbine mechanical system and DFIG with back-to-back converter models. Two mass-spring model is considered for wind turbine mechanical system of DFIG based WECS [20-23]. The DFIG back-to-back converters are modeled using vector control to achieve the independent control of active and reactive powers of DFIG based WECS. Fig. 2(a) and (b) shows the structure of Rotor Side Converter (RSC) and Grid Side Converter (GSC) of DFIG. In vector control, the stator voltage vector of DFIG is aligned with the synchronous reference frame q-axis. The RSC is constrained to control the torque and reactive power of DFIG based WECS; the GSC maintains the DC-link voltage and terminal voltage constant [21, 22]. The complete modeling of DFIG and its converter controllers can be found in author's previous work [22].

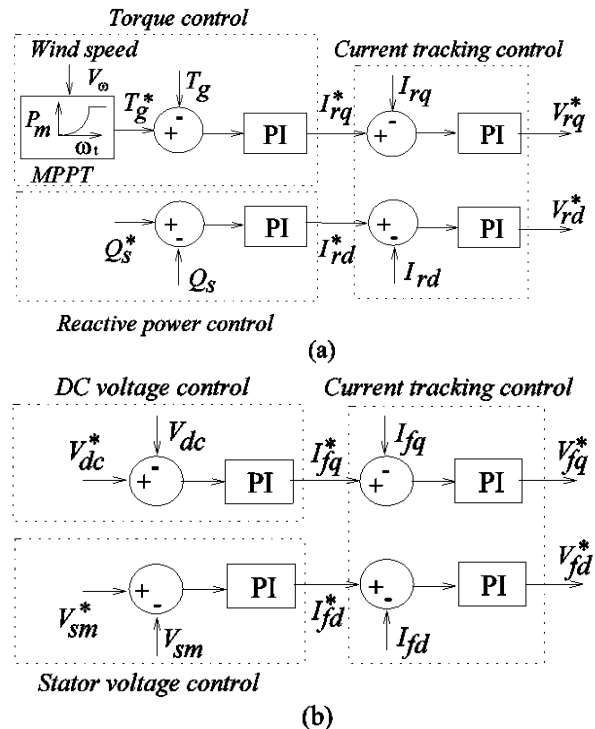


Fig. 2. (a) DFIG rotor side converter, (b) DFIG grid side converter.

## III. ADMITTANCE MODELING OF THE SYSTEM

In this section, we introduce a simple and general procedure to obtain the admittance model of the power system. Further, the proposed procedure is used to

obtain the admittance model of the test system described in Section-II.

#### A. Procedure to obtain the admittance model of a system

We describe the admittance model development of a system as a function of frequency in D-Q frame using admittance functions [10, 11]. The admittance model of the power system is computed viewing from a driving point. A Step-by-step procedure for admittance modeling is as follows:

*Step-1:* Split the power system into subsystems.

*Step-2:* Develop the model of the subsystems in MATLAB/Simulink using mathematical equations.

*Step-3:* Select an appropriate input and output variables of the subsystems to obtain the admittance function.

*Step-4:* Obtain the linear model and state space matrices of the subsystems with state model representation as,

$$[\Delta x'] = [A][\Delta x] + [B][\Delta u] \quad (1)$$

$$[\Delta y] = [C][\Delta x] + [D][\Delta u] \quad (2)$$

where  $[A]$ ,  $[B]$ ,  $[C]$ ,  $[D]$  are the state space matrices;  $x/u/y$  are state/input/output vectors, respectively.

*Step-5:* Obtain the admittance matrix of the subsystems by using the state model as,

$$[Y(s)] = [C](s[I] - [A])^{-1}[B] + [D] \quad (3)$$

$[I]$  is identity matrix. The admittance matrix,  $[Y(s)]$  of Eq. (3) is in DQ-frame and represented by,

$$[Y(s)] = \begin{bmatrix} Y_{DD}(s) & Y_{DQ}(s) \\ Y_{QD}(s) & Y_{QQ}(s) \end{bmatrix} \quad (4)$$

*Step-6:* Calculate the per phase admittance of the subsystems at a subsynchronous frequency using admittance matrix,  $[Y(s)]$  as,

$$Y(j(\omega_0 - \omega)) = \frac{1}{2} \left[ [Y_{DD}(j(\omega)) + Y_{QQ}(j(\omega))] - [Y_{DQ}(j(\omega)) - Y_{QD}(j(\omega))] \right] \quad (5)$$

*Step-7:* The series/parallel integration of admittance model of subsystems at the driving point of the power system gives the overall admittance model.

The procedure is useful to develop the admittance model of a large power system. Also, the overall admittance model obtained in Step-7 is used for frequency scanning studies.

#### B. Development of admittance model of the test system

The test system (shown in Fig. 1) is divided into subsystems as: synchronous generator with short line ( $Y_s$ ), DFIG based WECS with short line ( $Y_w$ ) and series compensated transmission line ( $Y_l$ ). Fig. 3 shows the admittance model of the test system (shown in Fig. 1).

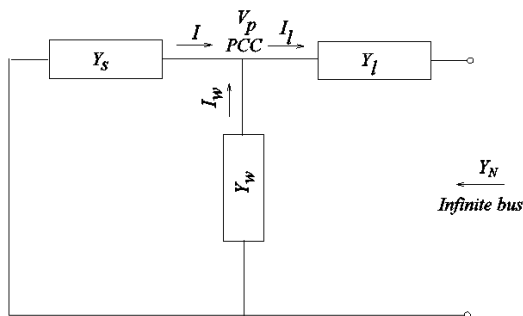


Fig. 3. Admittance model of the system viewed from infinite bus.

The overall system admittance ( $Y_N$ ) is obtained by the integration of individual admittance models. The admittance viewed from the infinite bus into the system is used for SSR screening studies. The admittance model of each subsystem is calculated using the admittance modeling procedure as follows:

**Calculation of admittance ( $Y_s$ ).** The state model of the synchronous generator with short line up to PCC is obtained by considering the input vector,  $u$  as internal bus voltage and output vector,  $y$  as resultant current ( $I$ ) (see Step-2 to Step-4 of admittance model procedure). From the state Eqns. (1) and (2), the admittance matrix is calculated (see Step-5). Using Eqn. (5) of Step-6, the per phase admittance ( $Y_s$ ) is calculated at subsynchronous frequency as,

$$Y_s(j(\omega_0 - \omega)) = \frac{1}{2} \left[ [Y_{sDD}(j(\omega)) + Y_{sQQ}(j(\omega))] - [Y_{sDQ}(j(\omega)) - Y_{sQD}(j(\omega))] \right] \quad (6)$$

**Calculation of admittance ( $Y_w$ ).** The admittance model of DFIG based WECS consists induction generator, back-to-back converter controllers, interfacing transformer and short line up to PCC. Using Eqns. (1) and (2), the small signal model is developed. Assuming that the voltage at PCC is considered as input vector,  $u$  and the current ( $I_w$ ) as output vector,  $y$  the admittance matrix is calculated using Step-5. From Eq. (5), the per phase admittance ( $Y_w$ ) at subsynchronous frequency is given by,

$$Y_w(j(\omega_0 - \omega)) = \frac{1}{2} \left[ [Y_{wDD}(j(\omega)) + Y_{wQQ}(j(\omega))] - [Y_{wDQ}(j(\omega)) - Y_{wQD}(j(\omega))] \right] \quad (7)$$

**Calculation of admittance ( $Y_l$ ).** The transmission line transients are represented with the lumped parameters [14]. The transmission line state model and admittance matrix (from Step-2 to Step-5) is obtained by assuming the input and output variables as infinite bus voltage and line current ( $I_l$ ), respectively. The per phase admittance ( $Y_l$ ) at subsynchronous frequency using Eq. (5) is given by,

$$Y_l(j(\omega_0 - \omega)) = \frac{1}{2} \left[ [Y_{lDD}(j(\omega)) + Y_{lQQ}(j(\omega))] - [Y_{lDQ}(j(\omega)) - Y_{lQD}(j(\omega))] \right] \quad (8)$$

**Overall admittance model.** The overall system admittance viewed from the infinite bus shown in Fig. 3 can obtain by the appropriate integration of individual admittance models. The expression representing system admittance model ( $Y_N$ ) at subsynchronous frequency is given by,

$$Y_N(j(\omega_0 - \omega)) = \left[ [Y_s(j(\omega_0 - \omega)) + Y_w(j(\omega_0 - \omega))]^{-1} + Y_l(j(\omega_0 - \omega)) \right]^{-1} \quad (9)$$

At a subsynchronous frequency,  $\omega = \omega_m$ , the system admittance function is represented as,

$$Y_N(j(\omega_0 - \omega)) = G_N(j(\omega)) + jB_N(j(\omega)) \quad (10)$$

where,  $G_N(j(\omega))$  and  $B_N(j(\omega))$  are the subsynchronous conductance ( $G_N^{sub}$ ) and susceptance ( $B_N^{sub}$ ) of the network, respectively. The developed admittance model is used to estimate the SSR frequency and damping of subsynchronous network mode. In Section-IV, we demonstrate the IGE of DFIG based WECS using admittance model based analysis and correlated with eigenvalue analysis.

#### IV. IGE ANALYSIS OF THE POWER SYSTEM WITH DFIG BASED WECS

In this section, the IGE analysis of the test system described in Section-II is presented using admittance model. Further, the results of admittance analysis are correlated with eigenvalue analysis and validated.

##### A. IGE analysis through admittance model

The admittance model based analysis is used to estimate the SSR frequency and the network conductance at various operating conditions.

**Estimation of SSR frequency.** Noting that, at resonance condition the imaginary part of the admittance/impedance function is equal or very close to zero [7, 23]. For the frequency range of interest, the SSR frequency at any operating point is estimated from the admittance function given by Eq. (10). At SSR frequency the imaginary part of Eq. (10) become zero (i.e.,  $B_N^{sub} = 0$ ) and real part provides the conductance ( $G_N^{sub}$ ) offered by the network at that frequency.

The frequency response of the system admittance model for various operating conditions is shown in Fig. 4. From Fig. 4, we noticed that the value of susceptance ( $B_N^{sub}$ ) become equal to zero at different frequencies for various compensation levels. At the zero crossing frequencies of ( $B_N^{sub}$ ), the peak values in conductance, ( $G_N^{sub}$ ) is observed. Accordingly, the SSR frequencies are estimated for  $X_c = 0.2, 0.4, 0.6$  and  $0.8$  p.u as 235.55, 176.99, 132.17 and 94.66 rad/sec, respectively (at  $V_w = 8$  m/s). Also noted that, at the SSR frequency the conductance ( $G_N^{sub}$ ) offered by the network is greater.

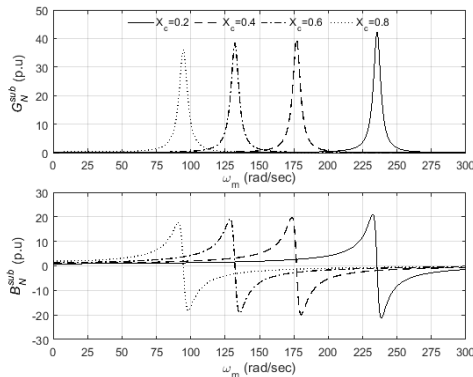


**Fig. 4.** Frequency response of admittance model for various compensation levels ( $X_c$ ) at wind speed,  $V_w = 8$  m/s.

**IGE analysis at various operating conditions.** The impact of DFIG based WECS on SSR frequency and network conductance is assessed using admittance model. For different operating conditions, the SSR frequencies and corresponding network conductance is calculated through frequency response of admittance model. Fig. 5 show the variation in SSR frequency and network conductance for change in wind speed ( $V_w$ ) and compensation level ( $X_c$ ). In Fig. 5, the vertical lines indicate the variation in SSR frequency and network conductance with change in wind speed at a compensation level. We observe that, at any

compensation level the network conductance increases with increase in wind speed.

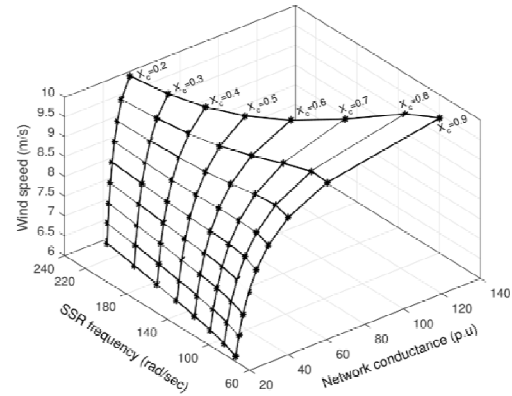


**Fig. 5.** SSR frequency and corresponding network conductance for various wind speeds ( $V_w$ ) and compensation levels ( $X_c$ ).

The SSR frequency decreases slightly with increase in wind speed. From Fig. 5, at any wind speed the SSR frequency reduces with increase in compensation level. Whereas, the increase in compensation level reduces the network conductance for low wind speeds and vice versa. Thus, the admittance analysis depicts that at high wind speeds and high compensation levels the conductance offered by the network to the subsynchronous current components is large.

##### B. IGE analysis through eigenvalue analysis

In the eigenvalue analysis, the complete model of the system shown in Fig. 1 is modeled and linearized at an operating point. The variation in subsynchronous network mode ( $NM^{sub}$ ) with change in operating conditions are tabulated in Table 1. The real and imaginary parts of the eigenvalues indicate the damping and frequency of  $NM^{sub}$ . The results in Table 1 indicate, at any compensation level with increase in wind speed, the damping of  $NM^{sub}$  reduces and frequency of  $NM^{sub}$  decreases slightly. At any wind speed the increase in compensation level reduces the  $NM^{sub}$  frequency. The damping of  $NM^{sub}$  increases at low wind speeds and decreases at high wind speeds with increase in compensation level. Results of eigenvalue analysis indicates, at high wind speeds and high compensation levels the damping of  $NM^{sub}$  reduces greatly.

##### C. Correlating admittance analysis and eigenvalue analysis

In relation to the admittance analysis with eigenvalue analysis, by comparing Fig. 4 and Table 1, the estimated SSR frequencies (235.55, 176.99, 132.17 and 94.66 rad/sec) are very close to the imaginary part of the eigenvalues shown in Table 1 for  $X_c = 0.2, 0.4, 0.6$  and  $0.8$  p.u at  $V_w = 8$  m/s. To correlate with the admittance analysis, the graphical representation of eigenvalue variation is shown in Fig. 6. In Fig. 6, the vertical lines indicate the variation real and imaginary parts of  $NM^{sub}$  with change in wind speed at a compensation level. The horizontal lines indicate the variation in real and imaginary parts of  $NM^{sub}$  with change in compensation level at a wind speed.

**Table 1: Eigenvalues of the subsynchronous network mode  $NM^{sub}$  for various wind speeds ( $V_w$ ) and compensation levels ( $X_c$ ).**

$V_w$ (m/s)	$X_c = 0.2$ p.u	$X_c = 0.3$ p.u	$X_c = 0.4$ p.u	$X_c = 0.5$ p.u	$X_c = 0.6$ p.u	$X_c = 0.7$ p.u	$X_c = 0.8$ p.u	$X_c = 0.9$ p.u
6	-3.324 ± j235.72	-3.562 ± j204.03	-3.804 ± j177.35	-4.055 ± j153.88	-4.329 ± j132.71	-4.653 ± j113.31	-5.081 ± j95.33	-5.7155 ± j78.56
6.5	-3.294 ± j235.67	-3.510 ± j203.96	-3.724 ± j177.26	-3.939 ± j153.77	-4.167 ± j132.58	4.434 ± j113.15	-4.796 ± j95.16	-5.354 ± j78.39
7	-3.253 ± j235.63	-3.442 ± j203.89	-3.621 ± j177.16	-3.792 ± j153.65	-3.966 ± j132.43	-4.171 ± j112.99	-4.458 ± j94.98	-4.933 ± j78.21
7.5	-3.199 ± j235.58	-3.354 ± j203.83	-3.491 ± j177.07	-3.611 ± j153.53	-3.724 ± j132.30	-3.857 ± j112.83	-4.064 ± j94.82	-4.450 ± j78.04
8	-3.132 ± j235.55	-3.244 ± j203.77	-3.330 ± j176.99	-3.391 ± j153.43	-3.436 ± j132.17	-3.490 ± j112.69	-3.610 ± j94.66	-3.902 ± j77.88
8.5	-3.048 ± j235.52	-3.108 ± j203.72	-3.135 ± j176.92	-3.127 ± j53.34	-3.094 ± j32.06	-3.063 ± j112.56	-3.092 ± j94.52	-3.288 ± j77.73
9	-2.943 ± j235.51	-2.943 ± j203.70	-2.896 ± j176.88	-2.810 ± j153.27	-2.692 ± j131.97	-2.570 ± j112.46	-2.504 ± j94.40	-2.603 ± j77.60
9.5	-2.803 ± j235.55	-2.725 ± j203.72	-2.600 ± j176.88	-2.427 ± j153.25	-2.216 ± j131.93	-2.000 ± j112.41	-1.839 ± j94.33	-1.844 ± j77.50
10	-2.555 ± j235.75	-2.424 ± j203.84	-2.216 ± j176.97	-1.952 ± j153.31	-1.647 ± j131.97	-1.337 ± j112.42	-1.085 ± j94.32	-1.002 ± j77.44

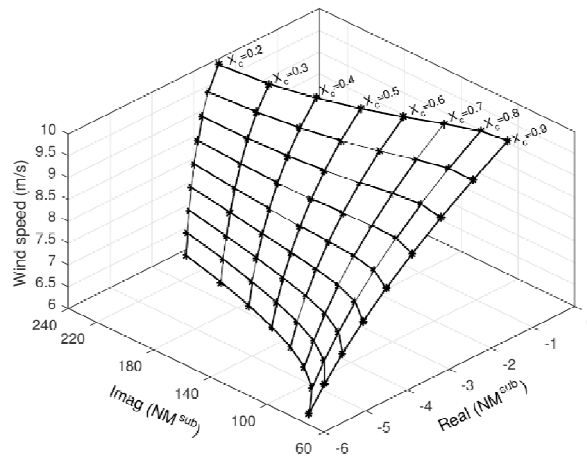


**Fig. 6.** Loci of eigenvalues of  $NM^{sub}$  for various wind speeds ( $V_w$ ) and compensation levels ( $X_c$ ).

The admittance analysis and eigenvalue analysis are correlated by comparing Fig. 5 and Fig. 6. For change in operating point, the variation of network conductance shown in Fig. 5 resembles the variation in real part of  $NM^{sub}$  shown in Fig. 6. For example, with the increase in wind speed the network conductance increases; also, the real part of  $NM^{sub}$  increases. Similarly, the SSR frequency shown in Fig. 5 is very close to the imaginary part of  $NM^{sub}$  shown in Fig. 6 at any operating point. From comparisons, the correlation between admittance analysis and eigenvalue analysis demonstrates: (1) the variation in network conductance of admittance analysis indicates variation in the real part of eigenvalues of  $NM^{sub}$  (i.e., damping), (2) the variation in SSR frequency of admittance analysis indicates variation in the imaginary part of eigenvalues of  $NM^{sub}$  (i.e., frequency). From the comparisons, the high conductance offered by the network to SSR frequency components indicate the less damping of  $NM^{sub}$ .

#### D. Discussion

The results of analysis methods show that, at high wind speeds and high compensation levels the conductance offered by the network to the subsynchronous components is large. When the multi-mass turbine-synchronous generator is connected to the series compensated transmission line, there is a possibility of torsional interactions. The severe torsional interactions may occur when the frequency of  $NM^{sub}$  is close to any one or more torsional modes of Multimass turbine synchronous generator. The admittance model analysis is useful to analyze the torsional interactions of multi-mass turbine synchronous generator.

#### V. CONCLUSION

This paper presents a simple and attractive procedure to obtain the admittance model of a system. The admittance model of the power system consisting DFIG based WECS is developed. Also, the admittance model based approach is used for the analysis of IGE at various operating conditions. Results of IGE through admittance analysis indicate that, the conductance offered by the network to the SSR frequency

components is large at high wind speed and high compensation levels. Further, the admittance analysis is correlated with eigenvalue analysis and validated. The correlations reveals that: (1) the variation in network conductance of admittance analysis indicates variation in the real part of eigenvalues of  $NM^{sub}$ , (2) the variation in SSR frequency of admittance analysis indicates variation in the imaginary part of eigenvalues of  $NM^{sub}$ . The results demonstrate that the high conductance offered by the network for the current components of SSR frequency indicates the severity of IGE.

## REFERENCES

- [1]. Harnefors, L., Bongiorno, M. and Lundberg, S. (2007). Input-admittance calculation and shaping for controlled voltage-source converters. *IEEE Transactions on Industrial Electronics*, 54(6): 3323–3334.
- [2]. Sun, J. (2011). Impedance-based stability criterion for grid-connected inverters. *IEEE Transactions on Power Electronics*, 26(11): 3075–3078.
- [3]. Céspedes, M. and Sun, J. (2013). Impedance modeling and analysis of grid-connected voltage-source converters. *IEEE Transactions on Power Electronics*, 29(3): 1254–1261.
- [4]. Fan, L. and Miao, Z. (2012). Nyquist-stability-criterion-based SSR explanation for type-3 wind generators. *IEEE Transactions on Energy Conversion*, 27(3): 807–809.
- [5]. Miao, Z. (2012). Impedance-model-based SSR analysis for type-3 wind generator and series-compensated network. *IEEE Transactions on Energy Conversion*, 27(4): 984–991.
- [6]. Amin, M. and Molinas, M. (2017). Small-signal stability assessment of power electronics based power systems: A discussion of impedance and eigenvalue based methods. *IEEE Transactions on Industry Applications*, 53(5): 5014–5030.
- [7]. Liu, H., Xie, X., Zhang, C., Li, Y., Liu, H. and Hu, Y. (2017). Quantitative SSR analysis of series-compensated DFIG based wind farms using aggregated RLC circuit model. *IEEE Transactions on Power systems*, 32(1): 474–483.
- [8]. Sun, K., Yao, W., Fang, J., Ai, X., Wen, J. and Cheng, S. (2020). Impedance modeling and stability analysis of grid-connected DFIG based wind farm with a VSC-HVDC. *IEEE Journal of Emerging and Selected Topics in Power Electronics*, 8(2): 1375-1390.
- [9]. Cheng, Y., Huang, S. H. and Rose, J. (2019). A series capacitor based frequency scan method for SSR studies. *IEEE Transactions on Power Delivery*, 34(6): 2135–2144.
- [10]. Liu, H., Xie, X., Gao, X., Liu, H. and Li, Y. (2018). Stability analysis of SSR in multiple wind farms connected to series-compensated systems using impedance network model. *IEEE Transactions on Power systems*, 33(3): 3118–3128.
- [11]. Padiyar, K. (1999). Analysis of Subsynchronous Resonance in Power Systems. Kluwer academic publishers.
- [12]. Kilgore, L., Ramey, D. and Hall, M. (1977). Simplified transmission and generation system analysis procedures for subsynchronous resonance problems. *IEEE Transactions on Power Apparatus and Systems*, 96(6): 1840–1846.
- [13]. Agrawal, B. and Farmer, R. (1979). Use of frequency scanning techniques for subsynchronous resonance analysis. *IEEE Transactions on Power Apparatus and Systems*, 341–349.
- [14]. Prabhu, N. and Padiyar, K. R. (2009). Investigation of subsynchronous resonance with VSC-based HVDC transmission systems. *IEEE Transactions on Power Delivery*, 24(1): 433–440.
- [15]. Janaki, M., Prabhu, N., Thirumalaivasan, R. and Kothari, D. (2014). Mitigation of SSR by subsynchronous current injection with VSC HVDC. *International Journal of Electrical Power Energy Systems*, 57: 287–297.
- [16]. Thirumalaivasan, R., Janaki, M. and Prabhu, N. (2013). Damping of SSR using sub-synchronous current suppressor with SSSC. *IEEE Transactions on Power systems*, 28(1): 64–74.
- [17]. Beza, M., and Bongiorno, M. (2020). Impact of converter control strategy on low-and high-frequency resonance interactions in power-electronic dominated systems. *International Journal of Electrical Power & Energy Systems*, 120:1-15.
- [18]. Liao, Y., Wang, X., Yue, X., and Harnefors, L. (2020). Complex-Valued Multifrequency Admittance Model of Three-Phase VSCs in Unbalanced Grids. *IEEE Journal of Emerging and Selected Topics in Power Electronics*, 8(2): 1934-1946.
- [19]. IEEE SSR working group. (1977). First benchmark model for computer simulation of subsynchronous resonance. *IEEE transactions on power apparatus and systems*, 96(5), 1565-1572.
- [20]. Ekanayake, J. B., Holdsworth, L., Wu, X. and Jenkins, N. (2003). Dynamic Modeling of Doubly Fed Induction Generator Wind Turbines. *IEEE Transactions on Power Systems*, 18(2): 803–809.
- [21]. Fan, L., Kavasseri, R., Miao, Z. L. and Zhu, C. (2010). Modeling of DFIG based Wind Farms for SSR Analysis. *IEEE Transactions on Power Delivery*, 25(4): 2073–2082.
- [22]. Velpula, S. and Rajaram, T. (2020). A simple approach to modelling and control of DFIG based WECS in network reference frame. *International Journal of Ambient Energy, (Article in press)*: 1–11.
- [23]. Wang, L., Xie, X., Jiang, Q., Liu, H., Li, Y. and Liu, H. (2015). Investigation of SSR in practical DFIG based wind farms connected to a series-compensated power system. *IEEE Transactions on Power systems*, 30(5): 2772–2779.

**How to cite this article:** Velpula, S. and Thirumalaivasan, R. (2020). Admittance Modeling of the Power System with DFIG based WECS for IGE Analysis. *International Journal on Emerging Technologies*, 11(4): 86–91.